Vietnam Journal of Catalysis and Adsorption
Tạp chí xúc tác và hấp phụ Việt Nam

Rh-supported ionic-liquid catalysts on TiO_2 for the conversion of Ethylene to propanol

Vu Tung Lam[1], Trinh Ba Hung[1], Le Minh Thang[1]

[1] School of Chemical Engineering, Hanoi University of Science and Technology, Hanoi, VIETNAM
*Email: thang.leminh@hust.edu.vn

ARTICLE INFO

ABSTRACT

Rhodium catalyst systems for hydroformylation has been researched widely in the literature. Using ionic liquid for rhodium-supported catalyst facilitates this reaction. In this work, TiO_2 support was first time used. From the FT-IR, EPR, and surface area analysis, the components of supported ionic liquid phase can be seen after the impregnation of ionic liquid into the support's porous structure. The main product for the ethylene conversion is propan-2-ol, as a subsequent hydrogenation product after hydroformylation. Pressure and temperature difference are evaluated to understand the influence on selectivity and product formation.

Introduction

For many years, hydroformylation has been one of the most used processes in the industry, converting alkenes to aldehydes and other products such as alcohol and amines... This reaction can be described as the addition of hydrogen (H) and the formyl (CH) group to the olefin, which is conveniently called hydroformylation [1]. Among many considerations, rhodium and cobalt easily stand out because of their high activity and high yield of desirable products [2]. During early developments, cobalt catalysts were applied in the hydroformylation of alkenes; however, relatively harsh conditions were needed, which can be as high as 200-300 bar and a temperature of 150-180°C [3].

An alternative catalyst using rhodium as an active site for the hydrogenation of alkenes was investigated in 1967 by Wilkinson [4]. It has been discovered that rhodium is a thousand times more active than cobalt, which resulted in the design of second-generation catalysts based on rhodium complexes. One of the first

industrial processes using rhodium complexes was the LPO Low-pressure oxo process. Reaction condition was reduced significantly, with operating pressure dropped to 10-50 bars and 120°C temperature [5]. The only downside of this generation catalyst was the ability to separate homogenous mixtures of catalysts and products. Biphasic rhodium-catalyzed hydroformylation was developed to create a water-soluble catalytic system, which is promising as the products and catalyst are separated into different layers of the system. On the other hand, creating an excellent biphasic system is a big challenge, as immobilizing catalysts in the water phase is tricky and hard to pull off [6].

Another consideration to the catalyst system was also considered, using ionic liquid as a "coat" to dissolve the active site in a porous structure, where reactants are diffusion through the layers of ionic liquid in and out. Therefore, the catalyst will be heterogeneous, while the active sites still fully work as a homogenous catalyst through the liquid phase [7]. Supported ionic liquid phase (SILP) catalyst concept results in the maintenance of high regioselectivity while providing a

more straightforward method to separate the catalysts from the products. Supported ionic liquid phase catalyst has been applied in hydroformylation using reactants ranging from 1-butene [8] to 1-hexene [9]. Although SILP catalysts have been applied on SiO_2, SBA-15, MCM-41, ZrO_2, Al_2O_3 supports, still, no study about the application of SILP on TiO_2 support for ethylene hydroformylation has been reported.

In our manuscript, supported ionic liquid phase catalysts were examined in the hydroformylation system, with variation in pressure and temperature, to understand the effects of reaction conditions.

Experimental

Materials

Triphenylphosphine TPP ((C_6H_5)$_3$P) (99%), fuming sulphuric acid H_2SO_4. $(SO_3)_x$ (68.0% free SO_3, toluene $C_6H_5CH_3$ were all from Sigma-Aldrich Chemical. Tri-n-octylamine (C_8H_7)$_3$N, 97%) was from Acros Organic. Sodium hydroxide (NaOH) (99%) and methanol (99.5%) were purchased from Xilong Scientific, where NaOH was dissolved in water and diluted to a 5% wt. NaOH solution.

To synthesize the TiO_2 support, titanium isopropoxide ($C_{12}H_{28}O_4Ti$, 99%) and toluene (99.5%) were from Merck. Pluronic P-123 (PEG-PPG-PEG) and sulfonate acid (H_2SO_4, 98%) were all purchased from Sigma-Aldrich. Isopropanol ((CH_3)$_2$CHOH, 99.7%) and acid citric monohydrate ($C_6H_8O_7.H_2O$, 99.5%) were all bought from Xilong Scientific.

Preparations of the catalyst

For SILP catalyst synthesis, all experiments were done in a vacuum system. In ligand synthesis, 5g Triphenylphosphine was added to a 500 ml flask, while 31mL Oleum slowly dropped. Afterward, the sulfonate reaction lasted approximately 170 hours, stirring and vacuum during the process. After being sulfonated, 100 mL of distilled water was added to lower the viscosity and increase diffusion ability for the next step. Subsequently, 24 mL Tri-n-octylamine was used to create an intermediate product for neutralization reaction, using 90 mL toluene (Merck) as a solvent. After that, the neutralization reaction used sodium hydroxide 5% until the pH of the mixture reached 5.5 - 6.5. After each pH level (2, 5, 6.5), the mixture was extracted to retrieve the tri-sulfonate triphenylphosphine phase using a pear-shaped

separatory funnel, separated mono-sulfonate, di-sulfonate, and tri-sulfonate triphenylphosphine at the bottom phase, respectively. The ligand triphenylphosphine trisulfonate-sodium was finally dried at 80°C, using methanol as a solvent.

The hydrothermal method was used to obtain the TiO_2 support, with Titanium isopropoxide as a precursor. Pluronic P-123 was used as a template-creator for TiO_2 and stirred with 100 mL of distilled water and 100 mL of isopropanol for an hour. In order to stabilize the mixture, 10,77g of acid citric monohydrate and 4 mL of sulfonate acid were added. After that, 62,5 mL TTIP was immediately added to the mixture using a micropipette, while 40 mL IPA was also used to avoid TTIP precipitating during the process. The solution was settled at 50°C in 24 hours. Following settling, the hydrothermal synthesis took place using an autoclave at 90°C for three days. Subsequently, the solution was washed, filtrated, dried at 90°C for 24 hours before grinding, and finally calcinated at 450°C in 5 hours.

Along with the newly-synthesis ligand and support, ionic liquid and rhodium are impregnated into support morphology, using methanol to dissolve into the pore structure of TiO_2. Methanol was distilled at 80°C, using zeolite Y as an adsorbent to separate water. As for the supporter, thermal-treating at 200°C for 3 hours removed the moisture, with the heating rate of 2°C per min to control evaporation rate, which can lead to morphology destruction if the rate is too fast. Synthesized-TiO_2, ligand TPPTS-Na$_3$, Rh(CO)$_2$(acac) dicarbonyl-acetylacetonato-Rhodium(I) and 1-butyl-3-methylimidazolium-octyl sulfate([BMIM][n-$C_8H_{17}OSO_3$]) were precious weighted and added into a flask, respectively. Next, distilled methanol was used to dissolve the mixture for 8 hours, followed by drying methanol similar to ligand synthesis.

Catalysts characterization

The FT-IR spectrum was determined by a JASCO 4600 equipment (Japan). The oxidation state of rhodium was investigated by a Bruker EMX-Micro EPR spectrometer, whereas the surface area was measured using a Micromeritics Gemini VII 2390 device.

Activity testing and calculation

A fixed bed hydroformylation system is used to evaluate the catalyst's activity. 0.5g catalyst was loaded into a 30cm stainless steel tube, which used an oven to reach the reaction temperature. The C_2H_4: CO: H_2 flow

ratio was 1: 1: 1. The outlet flow products were determined by a GC-FID detector using a Supel-Q 30m x 0.32mm column.

The product molar was calculated using a calibration standard.

Equation 1 was used to calculate the yield of the desirable products:

$$Yield \ (\%) = \frac{Molar \ of \ Ethylene}{Molar \ of \ product} * 100 \qquad (1)$$

The turnover frequency (TOF) was calculated based on the product yield and the molar of rhodium in the catalyst

$$TOF = \frac{F_{C_2H_4}*Yield}{100* \ n_{Rh}} \qquad (2)$$

In which,

$F_{C_2H_4}$ is the molar flow of C_2H_4 (mol/h).

n_{Rh} is the molar of rhodium in the catalyst.

Results and discussion

FT-IR spectrum of synthesized TPPTS-Na_3 ligand is presented in Figure 1. From the FT-IR spectrum of the ligand TPPTS, the strong broadband at 3450 cm^{-1} is assigned to the O-H stretching vibration of H_2O from moisture interference, which also makes an appearance at 1625 cm^{-1} as a bending vibration. A weak band at 3064 cm^{-1} occurs to be bending vibration of C-H from the benzene ring. Hence, the ring's medium stretching vibrations are observed at 1460 and 1404 cm^{-1}, respectively. On the other hand, a signature peak of TPPTS is the asymmetric stretching of the SO_3 group (S=O bond, precisely). The band is observed to split into multiple shoulder peaks around 1200 cm^{-1}, similar to other triphenylphosphine complexes, such as TPPTS-Eu, and TPPTS-Dy, respectively [10].
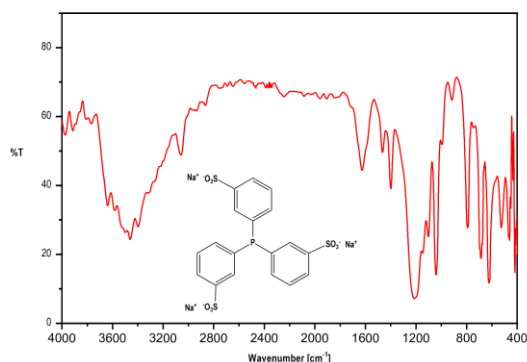
Figure 1: FTIR spectrum of the synthesized TPPTS-Na_3
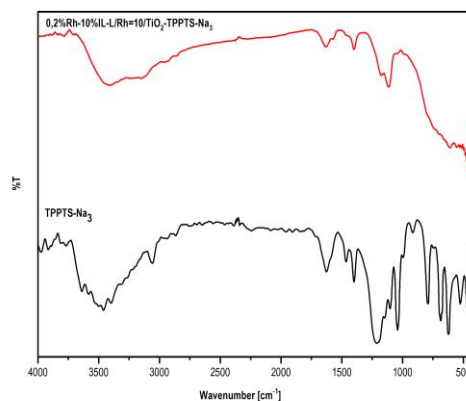
Figure 2: FT-IR spectrum of SILP catalyst and TPPTS-Na_3

However, in Figure 2, low concentration of individual components, combined with the high absorption of moisture, can also lower the transmittance of the ligand signature band, which appears as a medium band at 1200 cm^{-1} compared to strong broadband [11]. Despite overlapping other components, an absorption band at 540 cm^{-1} is assigned to the stretching vibration of the Ti-O bond, which can be explained due to support content higher than others [12].

The EPR spectra can also be used to examine the oxidation state of the catalyst, which is rhodium. In Figure 3, EPR spectra of SILP catalyst give the g factor value at 2.10, corresponding to the g factor of $[Rh^{II}(H)(CO)(PPh_3)_3]^+$ complex, which the ligand difference can cause a slight shift toward the g factor [13]. According to D. Menglet and Bond [13], the stable monomeric 17 electron rhodium (II) complex is switched back and forth to an 18 electron rhodium (III), which will ultimately cause rapid reductive elimination of H^+ resulting in the formation of $[Rh^I(CO)-(PPh_3)_3]^+$.
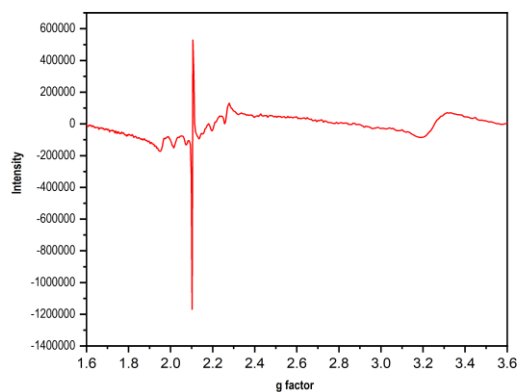
Figure 3: EPR spectrum of 0.2%Rh-10%IL-L/Rh=10-TiO_2-TPPTS-Na_3

The pore characteristic of different SILP catalysts and support is shown in Table 1.

Table 1: Surface area and pore characteristics of SILP catalyst supported by TiO_2

	Specific Area (m2/g)	Pore volume (cm³/g)	Average Pore Width (A°)
TiO_2	117.38	0.45	133.18
0,2%Rh - 10%IL - L/Rh = 10/TiO2, TPPTS - Na3	83.52	0.35	150.42
0,2%Rh - 30%IL - L/Rh = 10/TiO2, TPPTS - Na3	51.71	0.24	143.39

From Table 1, it is noticeable that after impregnating ionic liquid into the pore structure of TiO_2, the specific area dropped slightly. As ionic liquid loading increases, the pore volume and specific area are smaller than the supports.
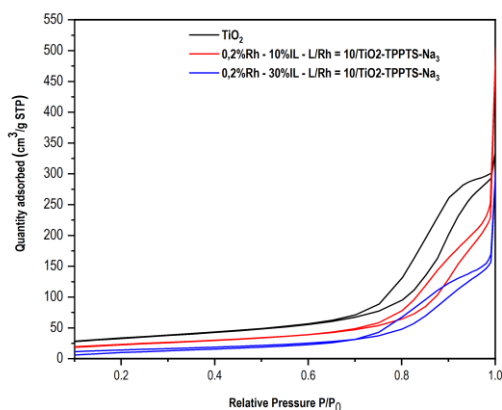
Figure 4: N2 adsorption-desorption isotherms of SILP catalyst and support
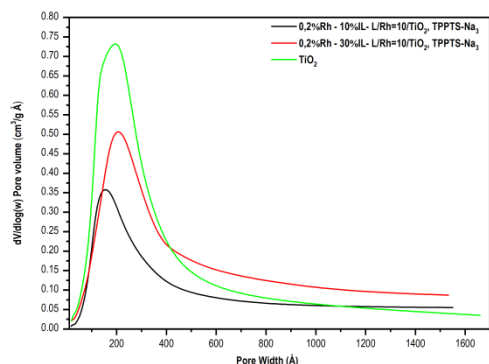
Figure 5: Pore size distribution of SILP catalyst and support

Figure 4 depicts the N2 adsorption-desorption isotherms for the supporter TiO_2 and SILP catalyst with different IL loading. All three plots fall under the type-IV classification. Additionally, TiO_2 and other SILP catalysts with different IL loading verify the mesoporous structure, showing a hysteresis loop after an approximate P/P0 =0.7. Meanwhile, Figure 5 compares the distribution of pore size obtained by the BET method. It is suggested that after loading IL, both catalysts' specific area decreases due to IL inside the mesoporous structure. However, Table 1 shows that average pore width tends to increase with increasing IL loading, implying that ionic liquid covers a smaller pore size, leading to average pore size rising.

Catalyst activity

The pressure effect on the product turnover frequency is shown in Figure 6. Product TOF increases with pressure and temperature, in agreement with the literature [14]. At atmospheric pressure, all catalysts show no activation over ethylene, even with a higher reaction temperature. While pressure is directly proportional to ethylene conversion, the temperature effect is somewhat contrary. The propan-2-ol yield was investigated at different temperatures as the ionic liquid decomposes at high temperatures. At 1 bar, ethylene shows barely any sign of oxidation to either propanal or propanol after 3 hours of reaction, but over at 7 bar, a higher transformation occurs. Despite that, propanal was not detected by our GC, but propan-2-ol instead.
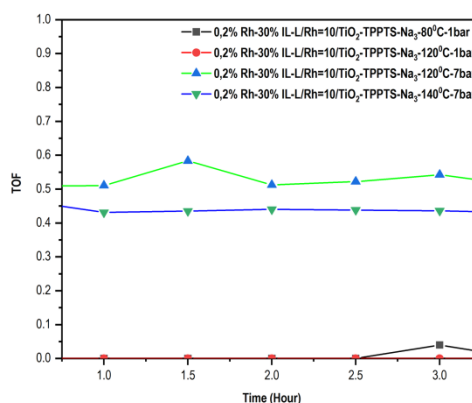
Figure 6: Propan-2-ol with time-on-stream over 0.5g powder 0,2%Rh - 10%IL - L/Rh = 10/TiO2, TPPTS - Na3, gas flow rate 60mL/min, at 1 bar and 7 bar

From Figure 7, propan-2-ol formation started slowly after 60 min time-on-stream at different reactions temperature. However, at 120°C, Rhodium SILP catalyst

displays low propan-2-ol selectivity during the early on-stream time but gradually increases over time, with a selectivity of 83.7% after 3.5 hours.
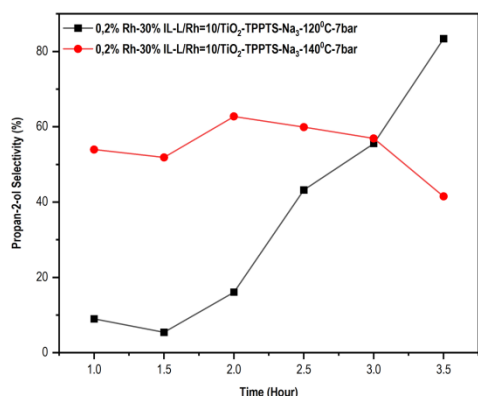
Figure 7: Propan-2-ol selectivity at different temperatures

In order to test the catalyst activity, the reaction temp was raised to 140°C. While showing a resemble to lower temperature during the first few hours, propan-2-ol selectivity slowly decreases after 2.5-3 hours, which can be depicted by the formation of ethane instead of propan-2-ol. According to the literature [15], increasing temperature favors the hydrogenation reaction rather than hydroformylation. This also agrees with the C_2H_4 conversion, as ethylene conversion at 140°C was stable while propan-2-ol selectivity was decreasing.
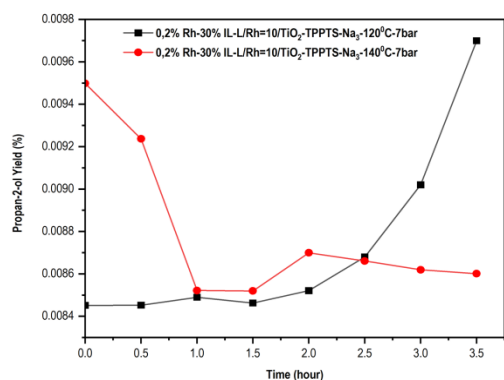
Figure 8: Propan-2-ol yield at different temperature

In Figure 8, it is clear that at 120°C, propan-2-ol yield increased gradually through time, but after 2 hours, the propan-2-ol yields became even higher. On the other hand, the yield at the start of the reaction at 140°C was significantly higher than at 120°C, but it decreased fast after the first hour of reaction. The yield was still higher, though the difference is minimal, but it dropped slightly over time. As ionic liquid becomes unstable at high temperatures, it can be assumed that

the preferable temperature at 7 bar for the reaction was 120°C.

Conclusion

This study investigated the properties of SILP catalyst and its difference to support, using various catalyst characterization methods. The catalyst activity testing also suggests that the more suitable temperature and pressure for the SILP catalyst are 120°C and 7 bar. Higher temperatures favor hydrogenation instead of hydroformylation and evaporate ion liquid, destroying the catalyst structure.

Acknowledgments

References

1. G. Jenner, Applied homogeneous catalysis with organometallic compounds 153 1–2 (1997) 254–255 https://10.1016/s0926-860x(97)80116-0
2. A. M. Trzeciak, Compr. Inorg. Chem. II (Second Ed. From Elem. to Appl. 6 (2013) 25–46. https://10.1016/B978-0-08-097774-4.00602-1
3. B. Zhang, D. Peña Fuentes, and A. Börner 8 1 (2022). doi: 10.1007/s40828-021-00154-x.
4. J. A. Osborn, G. Wilkinson, and J. J. Mrowca, Inorg. Synth. 10 (2007) 67–71. https://10.1002/9780470132418.ch12
5. C. P. Mehnert, R. A. Cook, N. C. Dispenziere, and M. Afeworki, J. Am. Chem. Soc. 124 44 (2002) 12932–12933. https://10.1021/ja0279242
6. B. M. Trost and S. L. Schreiber, Comprehensive Organic Sythesis Vol 1. 1993.
7. J. M. Marinkovic, A. Riisager, R. Franke, P. Wasserscheid, and M. Haumann, Ind. Eng. Chem. Res. 58 7 (2019) 2409–2420. https://10.1021/acs.iecr.8b04010
8. M. Schörner, P. Wolf, and M. Haumann, Green Chem. Eng. 2 4 (2021) 339–341. https://10.1016/J.GCE.2021.07.004
9. R. S. Kalb, Toward Industrialization of Ionic Liquids. (2020). https://10.1007/978-3-030-35245-5_11
10. C. Xinlan, L. Peng, Z. Lei, P. Hong, and Z. Lun 3 1

(1998) 86–91.

11. H. N. T. Ha, D. T. Duc, T. V. Dao, M. T. Le, A. Riisager, and R. Fehrmann Catal. Commun. 25 (2012) 136–141.
https://10.1016/j.catcom.2012.01.018

12. R. Ashiri, Vib. Spectrosc. 66 (2013) 24–29.
https://10.1016/j.vibspec.2013.02.001

13. D. Menglet et al., J. Am. Chem. Soc. 120 9 (1998) 2086–2089.

https://10.1021/ja973164x

14. V. I. Zapirtan, B. L. Mojet, J. G. Van Ommen, J. Spitzer, and L. Lefferts, Catal. Letters 101 1–2 (2005) 43–47.
https://10.1007/s10562-004-3747-8

15. N. Navidi, J. W. Thybaut, and G. B. Marin, CHISA 2012 - 20th Int. Congr. Chem. Process Eng. PRES 2012 - 15th Conf. PRES, p., 2012.